Submitted to Automatica 10/22/96

INVERSION-FREE DESIGN ALGORITHMS FOR MULTIVARIABLE QUANTITATIVE FEEDBACK THEORY: AN APPLICATION TO ROBUST CONTROL OF A CD-ROM[1]

Myoung Soo Park[2] Yossi Chait[3,4] Maarten Steinbuch[5]

ABSTRACT

This paper describes an application of multivariable Quantitative Feedback Theory (QFT) to a robust performance design of a compact disc mechanism. Robust control design is based on new QFT design algorithms which do not involve loop transmission inversion found in present QFT design algorithms. Their advantage is that even when the designer prefers inversion-based QFT loop shaping, the associated bounds can still be computed more efficiently using our inversion-free design algorithms. Plant uncertainty consists of parametric variations in the natural frequencies of dominant mechanical resonances and a variation in the interaction between the focus and radial loops. Robust performance specifications were given in terms of the multivariable closed-loop sensitivity function. The QFT controller was implemented in an experimental setup.

Key Words: multivariable control, robust control, CD ROM

---

[1]Research supported in part by an NSF grant CMS-9313764 at the University of Massachusetts. This support is greatly appreciated.
[2]Formerly: Research Assistant, MIE Dept., UMass, Amherst, MA 01003, USA, (email: mpark@ecs.umass.edu). Presently: Consultant, API, Inc, Mountain Farms Technology Park, Hadley, MA 01035-9547, USA.
[3]Associate Professor, MIE Dept., UMass, Amherst, MA 01003, USA. (email: chait@ecs.umass.edu).
[4]Author to whom all correspondence should be made.
[5]Member of the scientific staff, Philips Research Laboratories, P.O.Box 80.000, 5600 JA Eindhoven, The Netherlands. (email: steinbuc@natlab.research.philips.com).

INTRODUCTION

Figure 1 shows a schematic view of a compact disc mechanism. The mechanism is composed of a turn-table DC-motor for the rotation of the compact disc and a balanced radial arm for track-following. An optical element is mounted at the end of the radial arm. A diode located in this element generates a laser beam that passes through a series of optical lenses to give a spot on the information layer of the disc. An objective lens, suspended by two parallel leaf springs, can move in a vertical direction for focusing action.

Both the radial and the vertical (focus) position of the laser spot, relative to the track of the disc, have to be controlled actively. To accomplish this, the controller uses position-error information provided by four photo diodes. As input to the system the controller generates control currents to the radial and focus actuator, which both are permanent-magnet/coil systems. The control mechanism in a compact disc player can be represented by a linear, time-invariant, multivariable block diagram shown in Fig. 2. In system identification, only the differences between the radial and vertical track positions and the laser spot position can be measured (using an optical element). The generated signals are a radial error, ε_{rad}, and a focus error, ε_{foc}. Based on these measurements, the controller, G, feeds the system with the required control currents for each drive, ι_{rad} and ι_{foc}.

Two major sources of disturbances are track-position irregularities and external mechanical shocks. The track position specifications are based on standardization of CDs: the allowable radial deviation is 300 μm (eccentricity) and the allowable radial acceleration is 0.4 m/s^2. The external mechanical shocks are not specified. Measurements show that during portable use the spectrum of the disturbance signals includes the range of Hz to 150 Hz. The maximum allowable track-following error is 0.1 μm and the actuator current ι_{rad} should have a high roll-off above the bandwidth to prevent amplification of audible noise generated by the actuator. The control design problem here is based on a frequency domain formulation for the above specifications (Steinbuch *et al*., 1992).

DESIGN PROBLEM

Nominal Dynamics. Only modeling details necessary to explain the QFT control design procedure are described here. A complete description of the nominal model and uncertainty modeling is given in Steinbuch *et al*. (1992). Because the nominal plant response was obtained from closed-loop measurements, it effectively includes zero-order hold and digital computation effects. The frequency-response magnitudes of the identified, nominal plant are shown in Fig. 3. The identified 2x2 nominal plant, $P=\{p_{ij}\}$, consists of a 21^{st}-order model (two double integrators, 8 second-order modes with low damping and one fast real pole). The single input/output transfer functions in the nominal plant have right half-plane zeros: the significant one being in p_{11} at 2.0×10^4 rad/sec (3.2 kHz). Due to weak coupling, a similar right-half plane multivariable zero also appears in det[P]=0. The identified nominal plant is described by

$$\begin{bmatrix} \text{radial error} \\ \\ \text{focus error} \end{bmatrix} = \begin{bmatrix} p_{11} & p_{12} \\ \\ p_{21} & p_{22} \end{bmatrix} \begin{bmatrix} \text{radial current} \\ \\ \text{focus current} \end{bmatrix}$$

Uncertainty Description. On the basis of experience and physical reasoning the nominal plant was assigned two types of uncertainties. The first type, parametric, consists of ±2.5% variations about nominal values in each of the first three natural frequencies of the vibration modes at 0.8, 1.6 and 4.3 kHz. The second type, non-parametric, is related to the off-diagonal responses:

$$P = \begin{bmatrix} p_{11} & \varepsilon p_{22} + p_{12} \\ \\ \varepsilon p_{11} + p_{21} & p_{22} \end{bmatrix}, \quad \varepsilon \in [-0.1, 0.1] \qquad (1)$$

Note that the p_{ij} terms in (1) include parametric uncertainties (i.e., uncertain natural frequencies). These uncertainties define the CD's plant family denoted by $\mathcal{P}$.

Performance Specifications. Because QFT involves frequency-domain design, the specifications must be formulated in that domain. The frequency-domain formulation in Steinbuch *et al.* (1992) is used here. Note that since the only available measurements are the error signals, the performance specification are stated in terms of the sensitivity function, $S=(I+PG)^{-1}=\{s_{ij}\}$,

$$\left|s_{ij}(j\omega)\right| \leq \eta_{ij}(\omega), \; i,j=1,2, \quad \text{for each } P \in \mathcal{P} \tag{2}$$

and are shown in Fig. 4.

In QFT we compute performance bounds only within a finite bandwidth, in this design [0,200Hz]. In addition, we often use the maximum overshoot constraint, $|s_{ii}(\omega)|\leq 3$, $\omega\geq 0$, to generate gain-phase margins constraint on each loop

$$\left|1+p_{ii}^{2} g_{i}\right| \geq \frac{1}{3}, \omega \geq 0, \text{ for each } P \in \mathcal{P} \tag{3}$$

where $1+p_{ii}^{2} g_{i}$ are the denominators of the single-loop s_{ii} (see (5) below) The final requirements are that the nominal open-loop bandwidth in each loop should be kept below 1 kHz to avoid amplifying high frequency noises and audible responses of the actuators, and that the controller order be kept to minimum.

NEW DESIGN ALGORITHMS

During the past three decades, several techniques have been developed for multivariable control design within the framework of the QFT. These techniques focus on square nxn matrix transfer functions and diagonal controllers, and the design algorithms employ inversion of the loop transmission L(s)=P(s)G(s); for a recent review of various multivariable QFT design techniques see Horowitz (1991). In conventional QFT, the design problem is rigorously broken into an n-step sequential procedure. At each step, n single-loop QFT problems are solved for the n closed-loop transfer functions in that channel. In particular, the design algorithms involve the computation of QFT bounds.

QFT Bounds. Let some performance function F(s) involving the controller G(s) be given as well as a performance weight W(s), plant family $\mathcal{P}$, plant templates $\mathcal{P}_\omega$ and a nominal plant $P_0(s)$. For a fixed frequency ω, the *QFT bound* (for the nominal loop $P_0(s)G(s)$) is the set $P_0(j\omega)\mathcal{G}_\omega$ of complex number satisfying:

$$\left|F(j\omega)\right| \leq W(\omega), \quad \forall P(j\omega) \in \mathcal{P}_\omega$$
$$\Leftrightarrow$$
$$P_0(j\omega)G(j\omega) \in P_0(j\omega)\mathcal{G}_\omega$$

In this paper, we present new algorithms for computing QFT bounds in multivariable problems which do not use loop inversion. For this reason, we denote the multivariable QFT technique with the new algorithms as the ***direct technique***. These algorithms are more numerically efficient and can be used to complement present algorithms in some design problems.

Direct multivariable QFT employs the same sequential approach proposed in inversion-based techniques. It is constructive to briefly describe this concept now. Without loss of generality, we assume that the controller design proceeds in order from the first row to the last row. For the first row, suppose there exists a robust stabilizing controller g_1 such that $1+p_{11}g_1$ has stable zeros and achieves performance specifications at that loop for each $P\in\mathcal{P}$. Once g_1 is synthesized, suppose there exists a robust stabilizing controller for $1+p_{22}g_2$ (second row). However, because g_1 is known, before we design g_2, it can be embedded into the second row using the Gauss elimination technique. This design process of a single robust stabilizing g_i and subsequent elimination is then repeated n-1 times.

The New Algorithms. Using the same procedure described in Chait and Park, 1993, we can derive the appropriate relations for s_{ij} at each design step without use of explicit plant inversion as

$$s_{ij} = \frac{\alpha_{ji}^{L_1^{(i-1)}}}{\alpha_{ii}^{L_1^{(i-1)}} + \det[L_1^{(i-1)}]g_i} + \frac{\left[\sum_{k=i+1}^{n} - s_{kj}\,\alpha_{ki}^{L_1^{(i-1)}}\right]}{\alpha_{ii}^{L_1^{(i-1)}} + \det[L_1^{(i-1)}]g_i}, \qquad i,j = 1,2,\ldots,n \qquad (4)$$

where ($p_{ij}^{1} = p_{ij}$)

$$p_{ij}^{i} = p_{ij}^{1} - \sum_{k=1}^{i-1} \frac{p_{kj}^{k} p_{ik}^{k}}{1 + p_{kk}^{k} g_k} g_k \qquad (5)$$

$$L_1^{(i-1)} = \begin{pmatrix} 1+p_{11}g_1 & p_{12}g_2 & \cdot & p_{1(i-1)}g_{(i-1)} & p_{1i} & p_{1(i+1)} & \cdot & p_{1n} \\ p_{21}g_1 & 1+p_{22}g_2 & \cdot & p_{2(i-1)}g_{(i-1)} & p_{2i} & p_{1(i+1)} & \cdot & p_{2n} \\ . & . & . & . & . & . & . & . \\ p_{n1}g_1 & p_{n2}g_2 & \cdot & p_{n(i-1)}g_{(i-1)} & p_{ni} & p_{1(i+1)} & \cdot & p_{nn} \end{pmatrix} \qquad (6)$$

A at each i^{th} design step, the controller g_i is designed so that $1+p_{ii}^{i}g_i$ is stable for each $P \in \mathcal{P}$, and to meet performance specification in the i^{th} channel given in (2). The difficulty in trying to perform this set of single-loop designs is the explicit dependency in (4) on a set of yet to be designed closed-loop relations, s_{ij}, k=i+1,...,n, j=1,...,n. To facilitate a solution, we assume that there exist solutions to the multivariable robust performance problem, hence that

$$\left|s_{ij}(j\omega)\right| \le \eta_{kj}(\omega),\ k = i+1,\ldots,n,\ j = 1,2,\ldots n,\ \text{for all } P \in \mathcal{P},\ \forall\omega$$

Using the triangle inequality we simplify the above into the following n standard single-loop QFT problems at the i^{th} design step

$$\left|s_{ij}\right| \le \frac{\left|\alpha_{ji}^{L_1^{(i-1)}}\right| + \left[\sum_{k=i+1}^{n} \eta_{kj} \left|\alpha_{ki}^{L_1^{(i-1)}}\right|\right]}{\left|\alpha_{ii}^{L_1^{(i-1)}} + \det[L_1^{(i-1)}]g_i\right|} \le \eta_{ij}\ ,\ j = 1,2,\ldots n,\ \text{for all } P \in \mathcal{P},\ \forall\omega \qquad (7)$$

Note that the same concept of overbounding the s_{ij} terms in (4), necessary to derive (7), occurs also in inversion-based techniques. In Park (1994) it is shown that inversion-based algorithms can be obtained from direct algorithms by dividing all numerators and denominators in the latter by det[P]. The solution of a set of single-loop QFT problems and related computational issues are discussed in Chait and Yaniv (1993).

Numerical Efficiency. From a numerical computation stand point, direct algorithms employ det[P] and $p_{ij}(s)$ terms, while inversion-based algorithms employ plant inversion. Computing an LU factorization of P requires $n^3/3$ multiplications and $n^3/3$ additions, for *a total of $2n^3/3$ floating point operations*. The determinant is obtained from LU with only n multiplications, so we still have $2n^3/3$ floating point operations. If done carefully, the LU factorization can be used to get P^{-1} with $4n^3/3$ more operations, for *a total of $2n^3$ floating point operations*. These are only estimates and can be quite inaccurate for small n, say n<10 (Dongarra *et al.*, 1979). The general estimate is cubic polynomial in n. In addition, the number of operations is much larger for complex matrices (e.g., those representing the frequency response).

In MATLAB, for example, a good indication for the number of operations are *flops*. A random test gives the following results:

```
>> A = rand(100,100);

>> flops(0), det(A); flops
```

```
ans = 661650
>> flops(0), inv(A); flops
ans = 2039478
```

That is roughly $2/3 \times 10^3$ and 2×10^3, as predicted. Another test with a n=2 and complex frequency response gives:

```
>> A = [-1+i,.2+.1*i;.03+i,-55-i];
>> flops(0); det(A); flops
ans = 32
>> flops(0); inv(A); flops
ans = 260
```

Note that that MATLAB's inv(A) not only computes the inverse of A, it also estimates its condition to decide whether or not to display a warning message. The number of flops required for the condition estimate may depend upon A.

Taking into account that in control designs the inversion must be carried out over a large number of frequencies, the potential saving in terms of numerical computations is clearly seen from the above example.

Non-Minimum Phase Plants. A typical explanation used to justify plant inversion is that each equivalent diagonal plant element in the inversion-based algorithms, $1/q_{ii}(s)$ (recall $Q = P^{-1} = \{q_{ij}\}$), includes det[P] in its numerator. And since det[P] contains the plant's nonminimum phase zeros, one gains a "feel" for related design limitations which may not be seen directly from $p_{ii}(s)$. Moreover, in Horowitz (1992), Sec. 14.8, it is argued that limitations due to nonminimum phase zeros may be assigned to certain loops while completely avoided in all other loops. However, it is conceivable that if P has a nonminimum phase zero, $1/q_{ii}(s)$ may end up with not only that zero but also with an unstable pole. Indeed, in the CD-ROM model, the equivalent plant $1/q_{22}(s)$ has both a nonminimum phase zero at 2.0021e+4 and an unstable pole at 2.0396e+4. This implies that the inverse-based design should not start with the second loop, clearly an unnecessary limitation caused by the inversion.

Barring any numerical difficulties related to plant inversion, QFT bounds can be computed from (7) or the equivalent relation used in the inverse-based technique. QFT Loop shaping can then be performed using the actual nominal plant or the nominal plant in the inverse-based technique, by appropriately pre-multiplying $\mathcal{G}_{\omega}$ by the nominal plant We suggests that the bounds should be computed using the direct algorithms whose superior numerical efficiency has been established. The CD plant consists of 325 elements, hence numerical efficiency is an issue to be dealt with.

Finally, we note that in problems with $n \leq 3$ and low-order plants, one can compute P^{-1} by hand without difficulty, or even resort to symbolic programs (Sating *et al*., 1993). This approach is quite reasonable and was used successfully is numerous examples. However, in many plants, the dynamics include several resonances (e.g., mechanical or acoustical plants), a fact which significantly increases the plant order. However, the model identified based on the measured CD dynamics required at least a 21st-order model.

QFT CONTROL DESIGN

The first design step involves the radial controller g_1 to satisfy robust stability and the robust sensitivity performance specifications (the first loop). It is always recommended to first view the plant uncertainties in terms of templates, and those for p_{11}^{1} are shown in Fig. 6 at ω=[62.8, 251.3, 1257, 3142, 5404, 10120, 26890 and 62830] rad/sec. Note that Fig. 6 shows significant phase and magnitude variations at the three uncertain resonance frequencies. We used 375 plant cases to represent the uncertainty.

To compute QFT stability bounds, we used following inequality

$$\left|1+\frac{p_{11}+\det[P]g_2}{1+p_{22}g_2}g_1\right|\geq\frac{1}{3},\ \omega\geq 0,\ \text{for each } P\in\mathcal{P}$$

Because g_2 is yet to be designed, we considered its extreme values of g_2 in (5) (Yaniv, 1992), namely,

$$\begin{cases}\left|1+p_{11}g_1\right|\geq\dfrac{1}{3} & \omega\geq 0,\ \text{for each } P\in\mathcal{P}\quad (g_2\to 0)\\[2ex] \left|1+\dfrac{\det[P]g_1}{p_{22}}\right|\geq\dfrac{1}{3} & \omega\geq 0,\ \text{for each } P\in\mathcal{P}\quad (g_2\to\infty)\end{cases}$$

To compute the sensitivity bounds invoking (7) gave

$$\begin{cases}\left|s_{11}(j\omega)\right|=\dfrac{1+\left|\dfrac{p_{12}s_{21}}{p_{22}}\right|}{\left|1+\dfrac{\det[P]g_1}{p_{22}}\right|}\leq\dfrac{1+\left|\dfrac{p_{12}\eta_{21}}{p_{22}}\right|}{\left|1+\dfrac{det[P]g_1}{p_{22}}\right|}\leq\eta_{11}(\omega), & \omega\in[0,200],\ \text{for each } P\in\mathcal{P}\\[4ex] \left|s_{12}(j\omega)\right|=\dfrac{\left|-\dfrac{p_{12}}{p_{22}}\right|+\left|\dfrac{p_{12}s_{22}}{p_{22}}\right|}{\left|1+\dfrac{\det[P]g_1}{p_{22}}\right|}\leq\dfrac{\left|-\dfrac{p_{12}}{p_{22}}\right|+\left|\dfrac{p_{12}\eta_{22}}{p_{22}}\right|}{\left|1+\dfrac{\det[P]g_1}{p_{22}}\right|}\leq\eta_{12}(\omega), & \omega\in[0,200],\ \text{for each } P\in\mathcal{P}\end{cases}$$

Robust stability bounds and robust sensitivity bounds were computed the QFT Toolbox for MATLAB (Borghesani *et al.*, 1995). These bounds and the synthesized nominal loop are shown on the Nichols chart in Fig. 5.

Note that $L_{11,0}(s)=p_{11,0}(s)\ g_1(s)$ when $p_{11,0}(s)$ is p_{11} shown in Fig. 3. The controller is given by (rounded off)

$$g_1 = \frac{1.33\text{x}10^{10}(s^2 + 2.8\text{x}10^3 s + 4.6\text{x}10^6)(s+12.1)}{(s+2.9\text{x}10^5)(s^2 + 2.6\text{x}10^4 s + 3.8\text{x}10^8)(s+96)(s+1)}$$

The second design step is to design g_2 to satisfy the robust stability and robust performance specification while taking into account the known g_1. The plant used in the second design step, p_{22}^2, is defined by (5)

$$p_{22}^2 = p_{22} - \frac{p_{12}p_{21}g_1}{1+p_{11}g_1}$$

and its templates are shown in Fig. 8. Note that due to the high-gain g_1, the templates of p_{22}^2 exhibit larger variations around the three uncertain natural frequencies compared with the templates p_{22} alone. The plant p_{22}^2 is the open-loop plant seen by the controller to be designed.

Robust stability bounds were computed for

$$\left|1 + \frac{p_{22} + \det[P]g_1}{1+p_{11}g_1} g_2\right| \geq \frac{1}{3}, \quad \omega \geq 0, \text{ for each } P \in \mathcal{P}$$

$$\left|1 + \frac{p_{11} + \det[P]g_2}{1+p_{22}g_2} g_1\right| \geq \frac{1}{3}, \quad \omega \geq 0, \text{ for each } P \in \mathcal{P}$$

Robust sensitivity bounds were computed from (9)

$$\begin{cases} |s_{21}(j\omega)| = \left| \dfrac{\dfrac{-p_{21}g_1}{1+p_{11}g_1}}{1 + \dfrac{p_{22} + \det[P]g_1}{1+p_{11}g_1} g_2} \right| \leq \eta_{21}(\omega), \quad \omega \in [0,200], \text{ for each } P \in \mathcal{P} \\ \\ |s_{22}(j\omega)| \leq \left| \dfrac{1}{1 + \dfrac{p_{22} + \det[P]g_1}{1+p_{11}g_1} g_2} \right| \leq \eta_{22}(\omega), \quad \omega \in [0,200], \text{ for each } P \in \mathcal{P} \end{cases}$$

The robust stability bounds, robust sensitivity bounds and the synthesized nominal loop are shown on the Nichols chart in Fig. 6.

Note that $L_{22,0}(s) = p^2_{22,0}(s)\, g_1(s)$ where $p^2_{22,0} = p_{22} - \dfrac{p_{12}p_{21}g_1}{p_{11}+g_1}$ with p_{ij} shown in Fig. 3. The controller is given by (rounded off)

$$g_2 = \frac{2.9x10^4 (s+2713.2)(s+1622.2)}{(s^2 + 6.4x10^3 s + 2.9x10^8)(s+1)}$$

As expected, the robust stability bounds in the second loop are less "demanding" compared with those obtained in the first loop. Specifically, in the crossover frequency range, the first nominal loop is required to maintain less phase lag compared with the demand on the second nominal loop.

IMPLEMENTATION RESULTS

The experimental setup consisted of a compact disc player with an interface to a Digital Signal Processor (DSP) system. The actual implementation of the controller in the DSP has been carried out with dSPACE Cit-Pro software (dSPACE, 1989). Most problems occurring when implementing controllers involve problems such as scaling inputs and outputs to obtain the appropriate signal levels and to ensure that the resolution of the DSP is optimally used. These problems can be solved using the dSPACE software. The DSP system used is a Texas Instruments TMS320C25 16 bit processor with fixed point arithmetic. The Analog Digital Converters (ADC) are 16 bit and have a conversion time of 5 µs. The maximum input voltage is ± 10 V. The Digital Analog Converters (DAC) are 12 bit, have a conversion time of 3 µs and also operate within the range of ± 10 V. With the dSPACE software the following steps have been carried out: (1) a ramp-invariant discretization, (2) a modal transformation, (3) 1_1 scaling for the non-integrator states, (4) state scaling for the integrator states such that their contribution is at most 20 %; and (5) generation of DSPL code that can be downloaded to the DSP.

On the basis of the closed-loop relevant dynamics in the radial and focus loops, the discretization was done at a sampling rate of 27 kHz. The measured closed-loop sensitivity magnitudes are shown in Fig. 7. Note that in order to establish true robustness, the same controller must be tested on many compact disc players.

The observed peaks in $|s_{11}(j\omega)|$, especially in the 800-2000 Hz range, can be attributed to identification errors in the nominal plant. A detailed comparison between the identified radial loop and the measured data around those peaks revealed that the magnitudes matched well while the phases were off by only a few degrees. A single-loop QFT design was subsequently carried out and implemented in the radial loop using the raw experimental frequency response data (since with QFT the designer can work directly with complex data). The new design did not exhibit such peaks (Chait *et al.*, 1994).

CONCLUSIONS

This paper presented new multivariable QFT design algorithms with improved numerical efficiency and their application to control design of a compact disc mechanism. The application results indicate that QFT is an effective design tool for this class of systems having multivariable performance specifications and significant parametric plant uncertainty. Present research focuses on extending the new algorithms to non-diagonal QFT control design.

REFERENCES

Borghesani, C., Chait, Y. and Yaniv, O. (1995). *The QFT Toolbox for MATLAB*. The MathWorks, Inc., USA.

Chait, Y., and Yaniv, O. (1993). Multi-Input/Single-Output Computer Aided Control Design Using the Quantitative Feedback Theory. *Int. J. Robust and Nonlinear Control*, Vol. 3, pp. 47-54.

Chait, Y., and Park, M. S. (1993). Disturbance Rejection in Flexible Structures via the Quantitative Feedback Theory. *AIAA J. of Guidance and Control*, Vol. 15, No. 5. pp. 970-973.

Chait, Y., Park, M. S. and Steinbuch, M. (1994). Design and Implementation of a QFT Controller for a Compact Disc Player. *Journal of Systems Engineering*, Vol. 4, pp. 107-117.

dSPACE GmbH (1989). *DSPCitPro Software Package.* Documentation of dSPACE GmbH, Paderborn, Germany.

Dongarra, J.J., Moler, C.B., Bunch, J.R., and Stewart, G.W. (1979). *LINPACK User's Guide*. SIAM, Philadelphia.

Horowitz I. (1991). Survey of Quantitative Feedback Theory (QFT). *International Journal of Control*, 53(2), pp. 255-291.

Horowitz, I.M. (1992). *The Quantitative Feedback Design Theory (Vol. 1).* QFT Publications, 4470 Grinnell Ave., Boulder, Colorado, 80303.

Park, M. S. (1994). A New Approach to Multivariable Quantitative Feedback Theory. Ph.D. Thesis, University of Massachusetts, Amherst, MA.

Sating, R.R., Horowitz, I.M., and Houpis, C.H. (1993). *MIMO QFT CAD Package (ver. 2).* Air Force Institute of Technology (AU), Wright-Patterson AFB, OH.

Steinbuch, M., Schootstra G. and Bosgra O. H. (1992). Robust Control of a Compact Disc Player. *Proc. IEEE Conference on Decision and Control*, pp. 2596-2600.

Yaniv, O., (1995). Robust Feedback Synthesis for Margins at the Plant Input. *Automatica*, 31, pp. 333-336.

LIST OF FIGURES

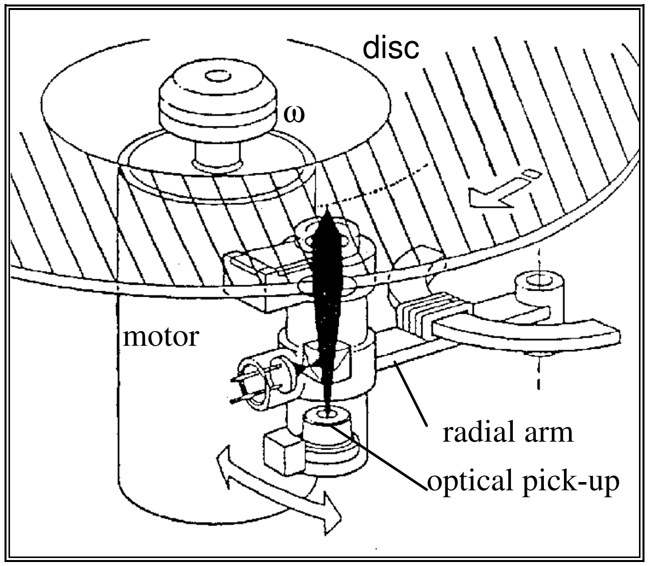

Figure 1

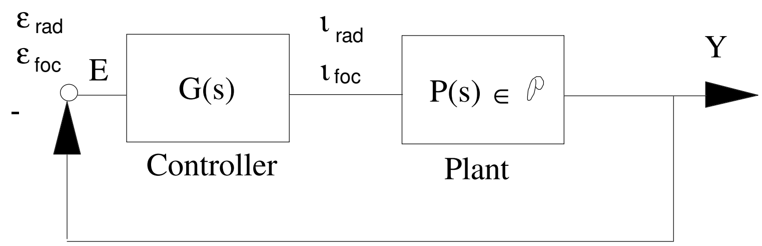

Figure 2

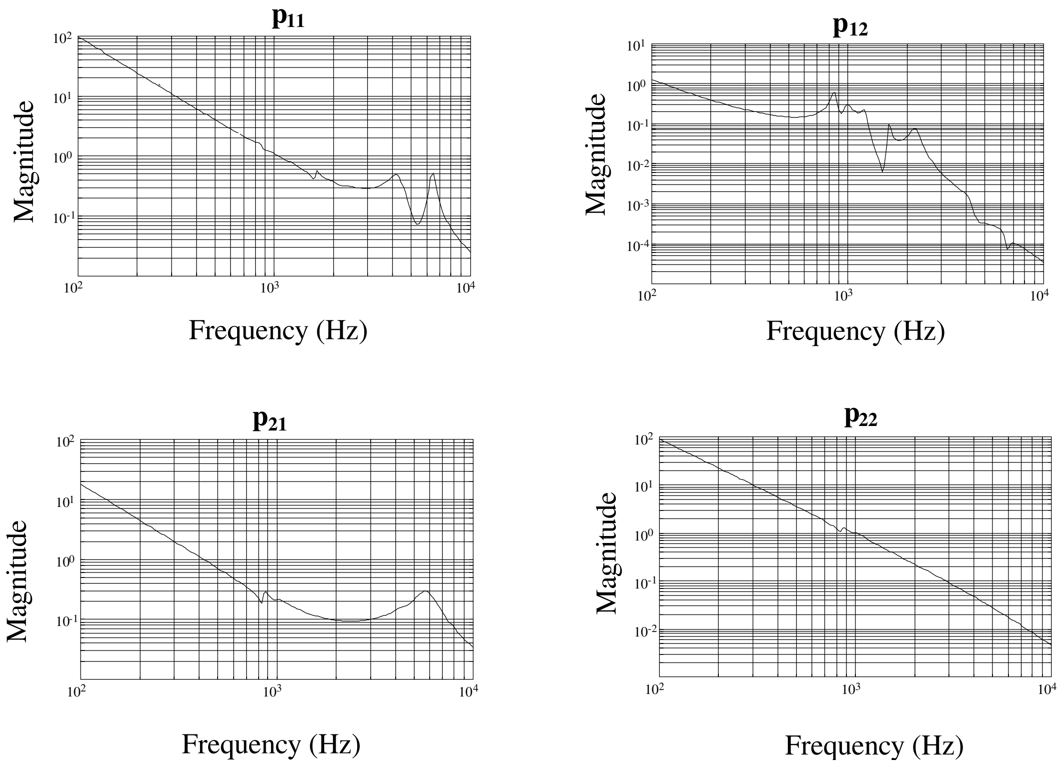

p_{11}
Magnitude
Frequency (Hz)
p_{12}
Magnitude
Frequency (Hz)
p_{21}
Magnitude
Frequency (Hz)
p_{22}
Magnitude
Frequency (Hz)

Figure 3

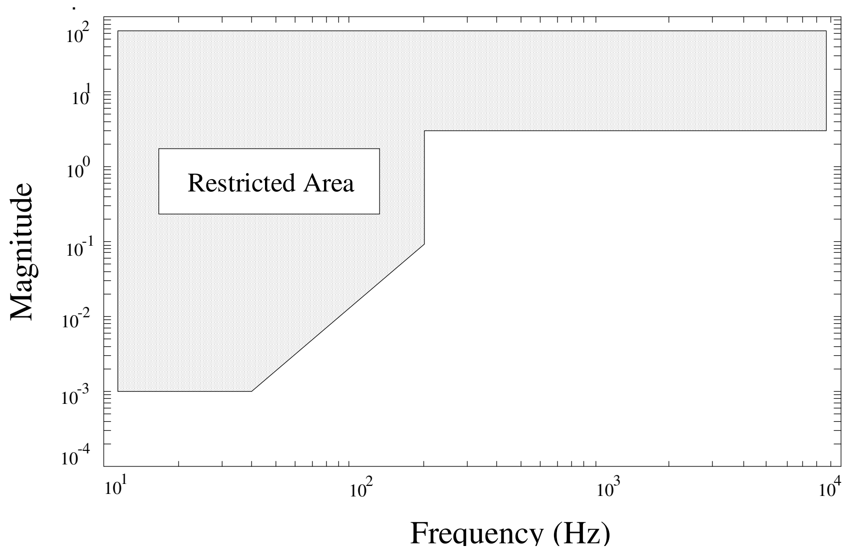

Figure 4

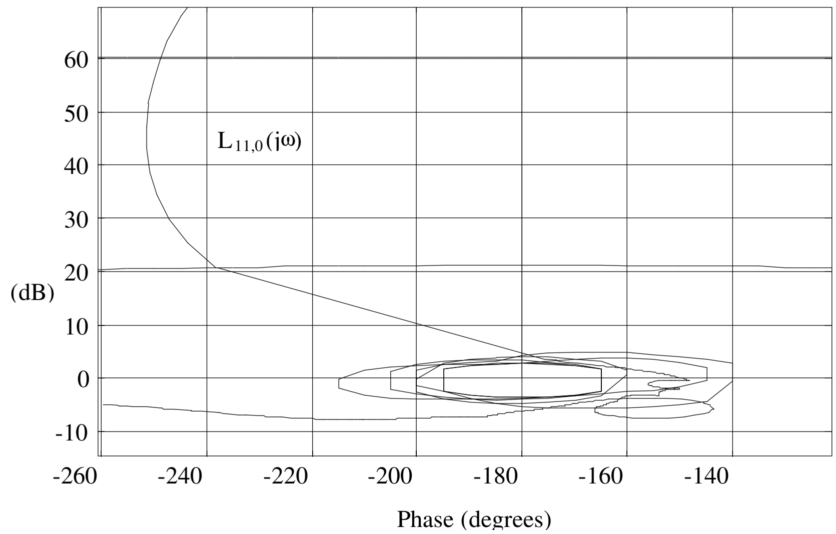
60
50
40
30
20
10
0
-10
(dB)
$L_{11,0}(j\omega)$
-260
-240
-220
-200
-180
-160
-140
Phase (degrees)

Figure 5

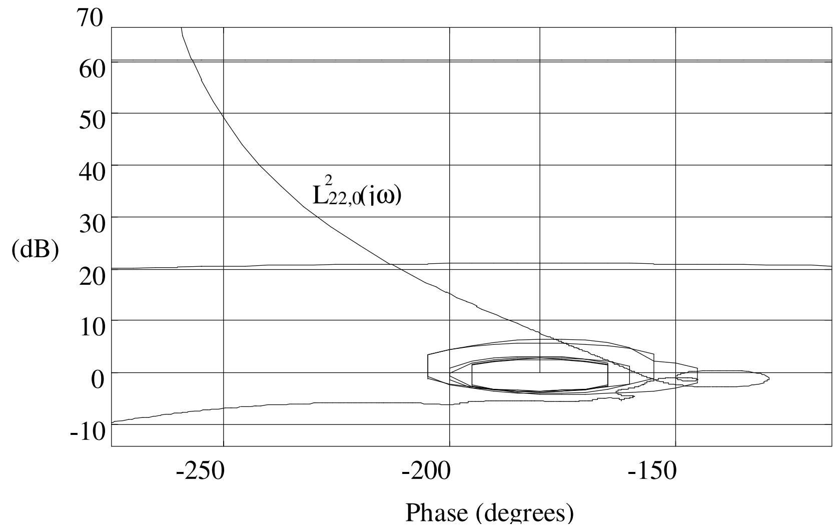
70
60
50
40
30
20
10
0
-10
(dB)
$L^2_{22,0}(j\omega)$
-250
-200
-150
Phase (degrees)

Figure 6

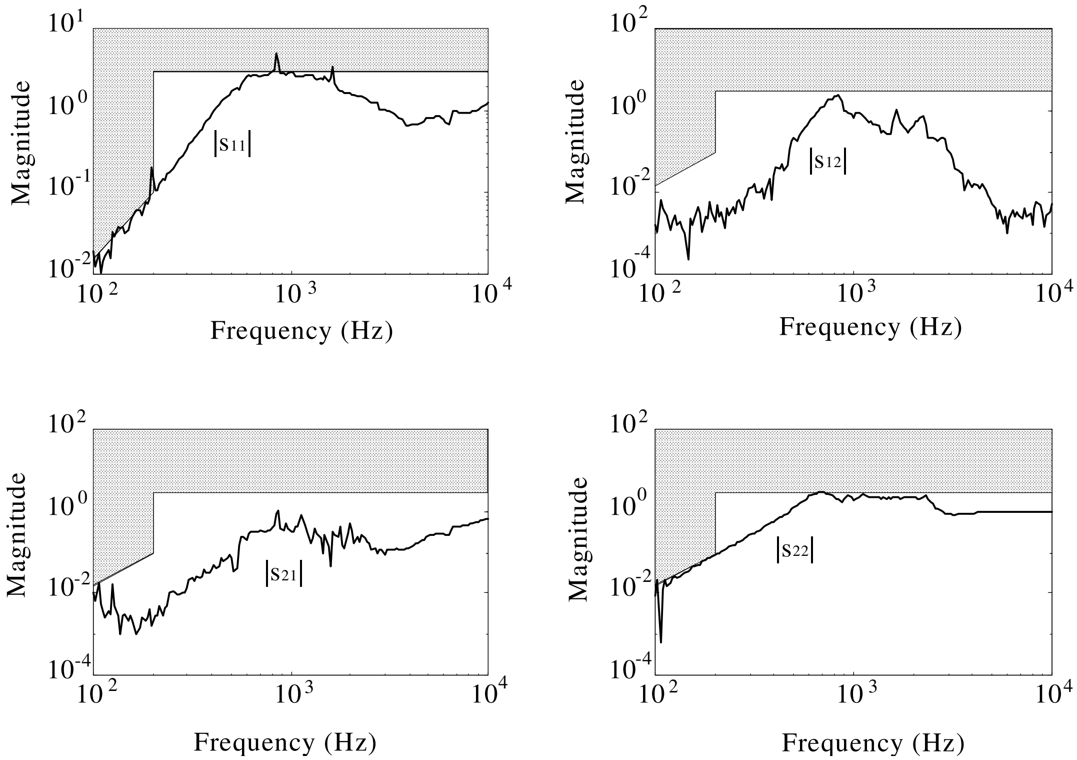

Magnitude
10^1
10^0
10^{-1}
10^{-2}
$|s_{11}|$
10^2
10^3
10^4
Frequency (Hz)
Magnitude
10^2
10^0
10^{-2}
10^{-4}
$|s_{12}|$
10^2
10^3
10^4
Frequency (Hz)
Magnitude
10^2
10^0
10^{-2}
10^{-4}
$|s_{21}|$
10^2
10^3
10^4
Frequency (Hz)
Magnitude
10^2
10^0
10^{-2}
10^{-4}
$|s_{22}|$
10^2
10^3
10^4
Frequency (Hz)

Figure 7